

# A comparison of overbank flow conditions in skewed and converging/diverging channels

J. Chlebek

*Ove Arup & Partners Ltd, Solihull, UK*

D. Bousmar

*Laboratoire de Recherches Hydrauliques, Service Public de Wallonie, Châtelet, Belgium*

*& Civil and Environmental Engrg Dept., Université catholique de Louvain, Louvain-la-Neuve, Belgium*

D.W. Knight & M. Sterling

*University of Birmingham, Birmingham, UK*

**ABSTRACT:** This paper investigates flows in compound channels with geometries which lie in-between purely prismatic and fully meandering channels cases, namely: skewed channel, symmetrically converging, and diverging channels. Experimental results from large sets of data produced by two research groups (University of Birmingham, UK and Université catholique de Louvain, Belgium) are analyzed and compared. Based on the water level, velocity and bed shear stress measurements, similarities in the flow behaviour are observed: (1) increased head losses due to the mass and momentum transfer; (2) homogenization of the velocity on contracting floodplains; and (3) increased velocity gradient on the expanding floodplains. Differences in the flow forcing from one subsection to another are also observed, resulting in significant differences in the flow distribution between main channel and floodplains.

*Keywords: Compound channels, Overbank flow, Skewed, Converging, Diverging channels*

## 1 INTRODUCTION

Flow in compound channels is complex and characterized by the transfer of momentum between the main channel and floodplain(s). This momentum transfer affects the total channel conveyance and should be accounted for in any flood management or engineering project. Two main processes of momentum transfer may be identified: (1) a turbulent exchange, linked to the shear layer development between the main channel and floodplain of a prismatic compound channel; and (2) a geometrical transfer, linked to the mass and flow exchanged between subsections, when the floodplain wetted area is no more constant (Bousmar & Zech, 1999).

There has been much work carried out in prismatic compound channels, including the work in the Flood Channel Facility, Wallingford, UK (FCF) in the 1980's and 1990's (Knight & Shiono, 1990). This resulted in an improved understanding of the turbulent processes in the shear layer, and in improved modelling methods. Fully meandering compound channels were also investigated in detail, in the FCF and at smaller scale elsewhere (see e.g. Sellin *et al.*, 1993; Spooner & Shiono, 2002).

However, to date, there has been little investigation into the change between prismatic and fully meandering channels. Such non-prismatic channels, including e.g. converging, diverging and skewed geometries (Fig. 1), are relevant to both researchers and engineers since the geometrical transfer processes may be isolated more easily and (2) such configurations may be encountered in floodplain planning projects as frequently as meandering geometries.

This paper reviews a large part of the existing experimental data for such non-prismatic channels, produced at the University of Birmingham and the Université catholique de Louvain. In particular, skewed, converging and diverging channels with similar cross-sectional shapes are selected. The experimental setup and main results are summarized. Finally, the flow in the different geometries are finally analyzed and compared.

## 2 PREVIOUS WORK

James & Brown (1977) are believed to be the first to investigate, in compound channels, the behaviour of flow when the floodplains are skewed. In their work, three skew angles of 7.2°, 11.0° and 24.0° were examined. Their main findings were

that the flow on the expanding floodplain accelerated whilst the flow on the converging floodplain decelerated. In addition, the overall resistance to the flow increased with the angle of skew.

Further skewed channel experiments were done at the FCF (Elliott & Sellin, 1990), with angle of 2.1°, 5.1° and 9.2°, and in a smaller scale flume by Ervine & Jasem (1995). This confirmed the reduced conveyance of a skewed compound channel, compared to a prismatic channel of similar cross-section. Ervine and Jasem (1995) found that the velocity in the main channel is approximately constant or decreases slightly downstream, implying that a process of substitution occurs along the channel, due to the cross-over flow.

Recently, Chlebek (2009) carried out a new experimental campaign on skewed channel, producing much more detailed data sets than the previously existing ones. This particular data will be used in this paper.

First experiments on converging compound channels with symmetrically narrowing floodplains were performed by Bousmar (2002), Bousmar *et al.* (2004a) and Rezaei & Knight (2009). These experiments highlighted the geometrical momentum transfer and the associated additional head loss. The Bousmar data set will also be presented in detail below.

Proust *et al.* (2006) also investigated an asymmetric geometry with a more abrupt convergence. Larger mass transfer and total head loss resulted from the higher convergence angle (22°). The analysis also showed that the head presented distinct evolutions in each subsection; the total head within the main channel decreases faster than that in the floodplain.

Lastly, Bousmar *et al.* (2006) investigated diverging compound channels, with symmetrically enlarging floodplains, in a similar setup to converging channels experiments of 2002. This data is also included in the analysis below.

### 3 EXPERIMENTAL SETUP

#### 3.1 Experimental program overview

The present paper associates data collected in two experimental flumes located at (1) the University of Birmingham, Birmingham, UK; and (2) the Université catholique de Louvain (UCL), Louvain-la-Neuve, Belgium. Brief details relating to both of these flumes are presented below.

Both flumes have quite similar cross-section, with a main-channel width and depth around 400mm and 50mm respectively, and two symmetrical floodplains 400mm wide. Also, main channel and floodplains in both flumes have smooth sur-

faces (PVC and coated plywood, respectively). Although the bed slope in Birmingham flume is twice the UCL one, these similarities enable easy comparison for non-dimensional variables.

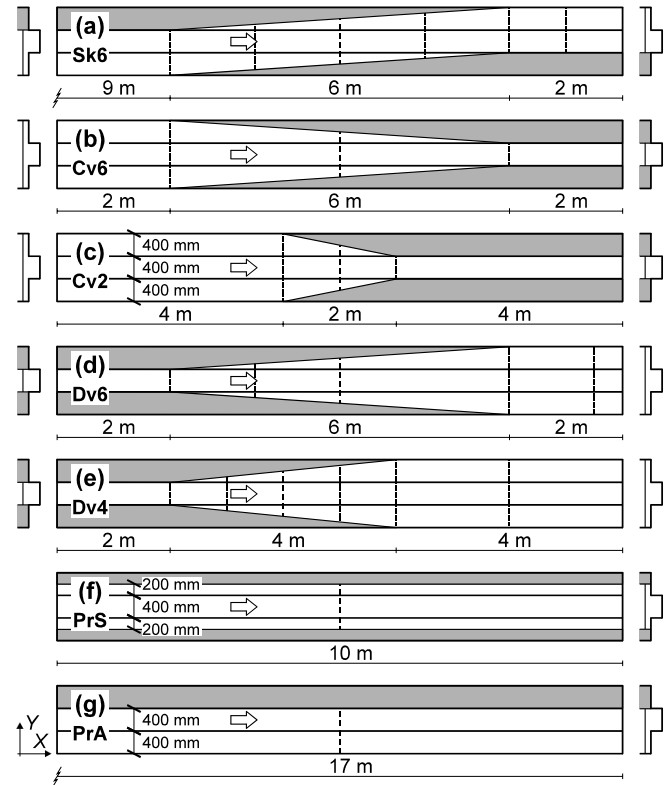


Figure 1. Configuration of the experimental flumes: (a) skewed; (b-c) converging; (d-e) diverging and (f-g) prismatic

Table 1. Experimental conditions.

Series <sup>(1)</sup>	Geometry	$Q$ (l/s) for $Dr =$ <sup>(4)</sup>			
		0.2	0.3	0.4	0.5
Sk6 <sup>(2)</sup>	Skew angle = 3.8° (6 m skewed reach)	16.2	21.4	29.6	43.4
Cv6 <sup>(3)</sup>	Converging angle = 3.8° (6 m narrowing reach)	10.0	10.0	12.0	20.0
Cv2 <sup>(3)</sup>	Converging angle = 11.3° (2m narrowing reach)	10.0	10.0	12.0	12.0
Dv6 <sup>(3)</sup>	Diverging angle = 3.8° (6 m enlarging reach)	12.0	12.0	16.0	16.0
Dv4 <sup>(3)</sup>	Diverging angle = 5.7° (4 m enlarging reach)	12.0	12.0	16.0	16.0
PrS <sup>(3)</sup>	Prismatic, symmetric (2 floodplains 200 mm)	9.9	13.4	27.6	
PrA <sup>(2)</sup>	Prismatic, g asymmetric (1 floodplain 400 mm)	18.0	21.0	30.1	43.8

<sup>(1)</sup> Cv: converging, Dv: diverging, Sk: skewed, Pr: prismatic, A: asymmetric, S: symmetric, 2/4/6: transition length in m

<sup>(2)</sup> University of Birmingham flume;

<sup>(3)</sup> UCL flume

<sup>(4)</sup> For Cv and Dv series, at mid-section, where floodplain width equals 200 mm.

As detailed in Table 1, work the Birmingham flume focused on a skewed channel geometry, with a non-prismatic section 6 m long (Fig. 1a). In this geometry, one floodplain width reduces, while the other increases. The total cross-section area remains almost constant, and a quasi-uniform flow is obtained.



Figure 2. Photograph of the University of Birmingham's experimental flume with a skewed geometry

The experiments in the UCL flume focused on symmetrically converging (Fig. 1b-c) or diverging (Fig. 1d-e) floodplains. In these geometries, the cross-section area is not constant and as such uniform flow is not obtained. The concept of relative depth,  $Dr$ , will be used throughout this paper and is defined as:

$$Dr = (H - h)/H \quad (1)$$

where  $H$  = total flow depth in main channel; and  $h$  = bank full depth. Each flume had a tailgate which was adjusted to ensure that  $Dr$  could be fixed at given values in the mid-section, where both floodplains have the same width of 200 mm. This enables comparison of the flow structure in a similar cross-section, with the similar flow depth, for different geometries.

Ancillary experiments were performed in reference prismatic geometries (Fig. 1f-g), corresponding either to the mid-section quoted above or to the entrance/outlet section of the skewed geometry.

In the subsequent sections, the experimental cases will be named with a three position label SSS/DD/QQ, where SSS = Series code as defined in Table 1; DD = relative flow depth  $Dr$ ; and QQ = discharge (l/s).

### 3.2 University of Birmingham flume

The University of Birmingham flume has a total length of 18 m, a depth of 400 mm and a 398 mm wide main channel which is 50 mm deep (Fig. 2). There are two floodplains which are each 398 mm wide. The flume has a bed slope of  $2.003 \times 10^{-3}$ . This flume has been used to study a number of possible channel configurations including prismatic channels with symmetrical or asymmetrical floodplains (Atabay, 2001), non prismatic flood-

plains (Rezaei, 2006) and skewed floodplains (Chlebek, 2009).

All of the experiments were carried out with rigid boundaries. The non-prismatic geometries were built using movable vertical walls on the floodplains (Fig. 2). The length of the upstream prismatic reach (Fig. 1a, g) was sufficient to ensure complete flow development.

Discharges were measured using a Dall tube, a Venturi meter and an Electromagnetic flow meter. Both local and depth averaged velocities were measured with a mini-propeller meter together with boundary shear stress (using a Preston and Pitot Tube arrangement).

In the non-prismatic sections, the channel had a total of 6 measuring sections; one at the start of the transition, three intermediate sections, one at the end and one 1m downstream of the end of the transition (Fig 1a).

Surface water level data was taken at regular intervals along the entire length of the flume using a pointer gauge, which was fixed onto an instrument carriage which could be read to 0.1 mm. In the skewed channel experiments, the normal depth was set upstream of the transition by adjusting the three tailgates. The actual relative depths corresponding to the discharges listed in Table 1 were fixed to  $Dr = 0.205, 0.313, 0.415$  and  $0.514$ .

Further details on the measuring instruments, procedures, and full data results may be found in Atabay (2001), Rezaei (2006) and Chlebek (2009).

### 3.3 Université Catholique de Louvain flume

The UCL tilting flume has a total usable length of 10 m. The useable width equals 1.2 m which includes a 400 mm wide main channel (50 mm deep) and two floodplains each 400 mm wide. The bed slope was fixed at  $0.99 \times 10^{-3}$ . This flume has been used to study notably converging (Bousmar, 2002; Bousmar *et al.*, 2004a) and diverging geometries (Bousmar *et al.*, 2006).

Again, non-prismatic sections were built using movable vertical walls. As the upstream length was not sufficient to ensure proper flow development and discharge distribution between subsections, the upstream tank was separated into three parts to control the actual flow distribution between main channel and floodplains (Bousmar *et al.* 2005).

Discharges were measured using an Electromagnetic flow meter. Water levels and local velocities were recorded using an automated point gauge and a Pitot tube connected to a differential pressure sensor, respectively. The velocity direction was recorded using a micro-vane. All those instruments were mounted on an automatic dis-

placement trolley. Additional surface velocity data were recorded using digital imagery. Measurement sections are located on Figure 1b-e.

Further details on the measurement instruments and procedures, and full data results may be found in Bousmar (2002), Bousmar *et al.* (2004a, 2004b, 2006).

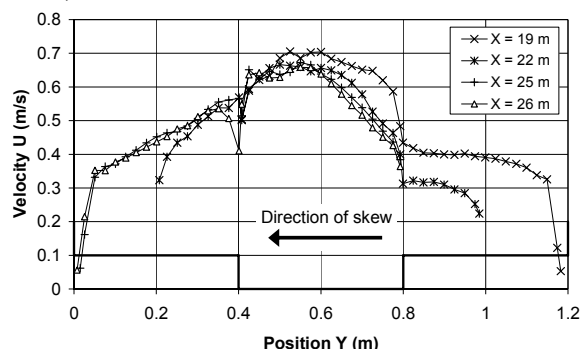


Figure 3. Sk6/03/21: Lateral distributions of streamwise depth-integrated velocity, at different cross-sections

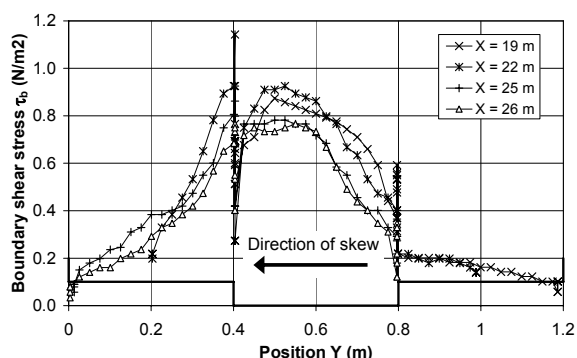


Figure 4. Sk6/02/16: Boundary shear stress distribution

## 4 KEY FINDINGS

### 4.1 Skewed channels

The skewed channel geometries, Sk6, were studied in detail by Chlebek (2009) and Chlebek & Knight (2008).

Using the stage-discharge data for the Sk6 series, a line of best fit was obtained mathematically in the form of a simple power function:

$$H = 0.5587 Q^{0.5325} \quad (2)$$

When compared to the asymmetric prismatic channel data (PrA series), the flow resistance is found to be slightly higher in the skewed channel. This highlights the effect of flow and momentum transfer between subsections.

It was found that water level variations throughout the transition were highly non-linear (see Fig. 10). The water surface profile followed that of the bed slope until the skewed transition begins. At the start of the transition, the water depth rises over the length of the 6 m skewed transition before coming back towards the normal

depth downstream. The rising water level has a marked effect on the velocity data.

Figure 3 shows typical depth-integrated velocity profiles. From these data the following observations were made:

- The maximum velocity moves from the centreline (where the velocity reaches a maximum in prismatic channels) to a location left of the centreline in the direction of skew.
- The velocities in the left hand floodplain (the receiving floodplain) are always greater than those on the right hand floodplain (the giving floodplain). Velocity on the left floodplain is up to 0.17 m/s greater than on the right one. However, as the water depth increases the difference between the right and left floodplains lessens.
- The velocity peaks slightly on the receiving floodplain at the interface between the main channel and floodplain. At this location, the peak is approximately 50 % larger than mean velocity on the left floodplain. Conversely, the velocity dips at the interface of the right/giving floodplain and main channel.
- The average velocity in the channel decreases through the transition due to the increasing water level caused by the increasing lateral mixing. The section average velocity decreases by approximately 0.04 m/s between  $X = 19$  m and  $X = 26$  m regardless of experiment.
- Using the velocity data, the discharge in each zone (floodplains and main channel) of the channel was estimated (see Fig. 13). Generally, the percentage of area in the main channel tends to be lower than the corresponding discharge. Conversely, in the floodplains, the percentage of area tends to be greater than the percentage discharge. As the depth increased ( $Dr > 0.313$ ), the agreement between the percentage area and discharge increases.

Figure 4 shows typical boundary shear stress distribution, which was measured indirectly using Preston tubes. This data is useful for a number of reasons. In the context of the current work it: (1) enables force balances along the channel to be examined; (2) provides excellent data for the calibration of numerical models and (3) can indicate the location of secondary flow cells. Examining this data, it can be observed that there is a peak at the interface of the main channel and left hand floodplain. The peak at this location can be up to twice that of the section average boundary shear stress for the lowest flow depth ( $Dr = 0.205$ ). At the highest flow depth ( $Dr = 0.514$ ), the peak approximately equals the section mean. This peak appears as it is located in a particularly turbulent region where the floodplain is receiving cross-over flows.

## 4.2 Converging channel

The converging channel geometries Cv6 and Cv2 were studied in detail by Bousmar (2002) and Bousmar *et al.* (2004a).

Typical water surface profiles for Cv2 and Cv6 series are shown on Figure 10. Before entering the non-prismatic section, a M1 water profile is observed, as the flow accumulates potential energy to pass the contraction. In the non-prismatic section, the flow accelerates strongly, resulting in a plunging water profile.

Figures 5 & 6 show typical depth-averaged streamwise velocity profiles. From these data the following observations were made:

- Due to the acceleration, the mean velocity increases in the downstream direction.
- Due to the convergence, the velocity is almost constant across the whole floodplain width. There is no velocity increase near the interface, as usually observed in the shear layer of a prismatic compound channel.
- Analysis of instantaneous surface velocity fields revealed that the large vortices with vertical axis observed in the shear layer of a prismatic compound channel are washed out in the converging section (Bousmar *et al.*, 2004b)
- When the relative flow depth increases, the velocity profile becomes flatter, with a floodplain velocity almost equal to the main-channel one at  $Dr = 0.5$ .
- For a given flow depth in the mid-section ( $X = 5$  m), the normalized velocity profile is similar for different discharges, and also for different converging angles.

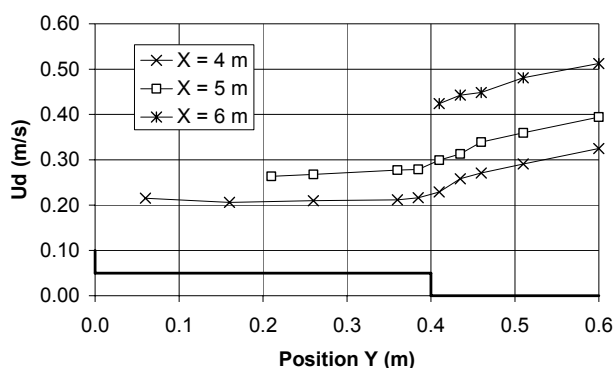


Figure 5. Cv2/03/12: Lateral distributions of streamwise depth-integrated velocity, at different cross-sections (half section)

The flow structure was summarized as depicted on Figure 7: (1) a transverse current is generated from the floodplain to the main channel due to the narrowing floodplains; (2) as these currents enter the main channel, they plunge towards the channel bottom; and (3) helical flows result in the inbank part of the main channel.

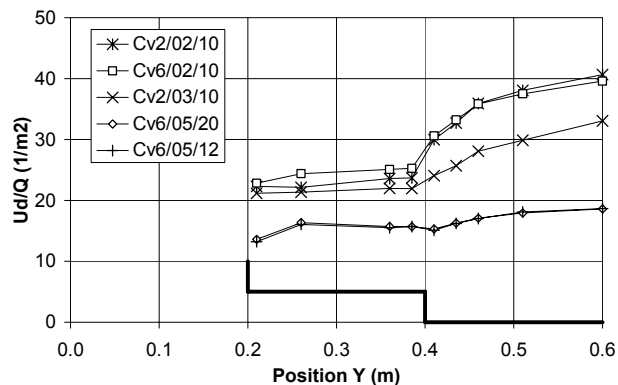


Figure 6. Cv2 & Cv6 series: Lateral distribution of depth-averaged velocity, normalized by the discharge, in the mid-section ( $X = 5$  m)

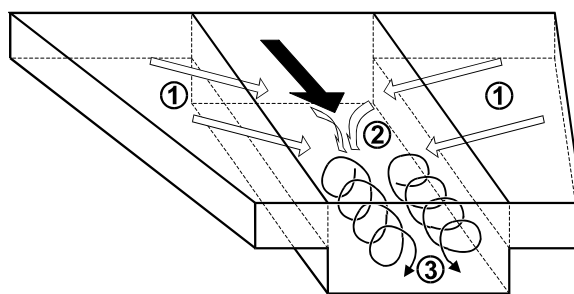


Figure 7. Schematic view of the flow structure in a converging compound channel.

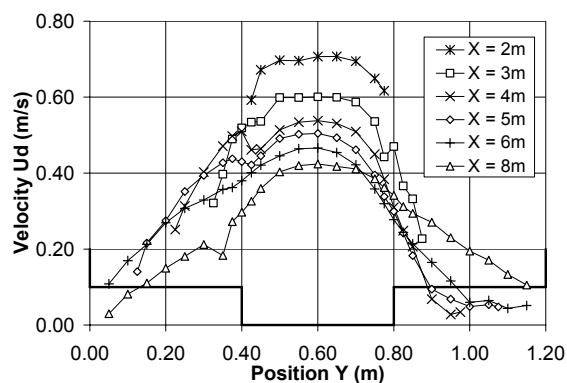


Figure 8. Dv4/03/16: Lateral distributions of streamwise depth-integrated velocity, at different cross-sections

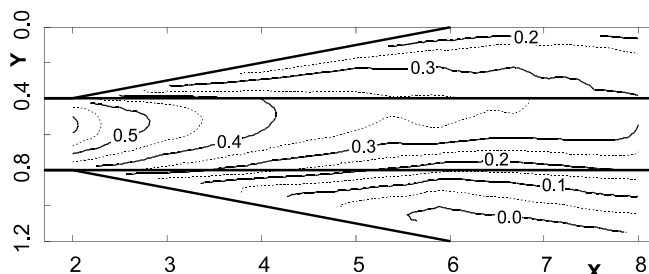


Figure 9. Dv4/05/20: Depth-averaged velocity field, obtained from digital imaging (velocity labels in m/s)

The momentum balance analysis of the converging flows highlighted the significant momentum transfer associated with the mass transfer through the interface. Additional head losses due to these transfers were found in some cases to be

equal to the friction losses in a prismatic case with the same cross-section and discharge.

### 4.3 Diverging channel

The diverging channel geometries Dv6 and Dv4 were studied in detail by Bousmar *et al.* (2006).

Contrary to the converging cases, the water profiles in the diverging geometries are found to rise in downstream direction, due to the deceleration (Fig. 10).

Figure 8 shows typical depth-averaged streamwise velocity profiles. From these data the following observations were made:

- Due to the deceleration, the mean velocity decreases in downstream direction.
- The velocity presents a very strong gradient on the whole floodplain width, with values close to zero along the lateral bank, and values close to the main-channel ones at the interface.
- There is a significant difference in the flow distribution between left and right floodplains. As illustrated in Figure 9, the flow presents strong instabilities due to its expansion. For the larger discharges, like the one depicted, some recirculation areas may even be observed along the floodplain banks.
- Due to these instabilities, the similarity between the normalized velocity profile at different discharges for a given flow depth in the mid-section ( $X = 5$  m) is less clear than in the converging cases.

Momentum and energy balance analysis again revealed increased head losses in the non-prismatic reach. Moreover, the local specific energy was found to evolve in a different way between the main channel and the floodplain, where it is even found to increase along a significant part of the non-prismatic section.

## 5 COMPARISON BETWEEN SKEWED AND CONVERGING/DIVERGING CHANNELS

Although the geometries of skewed and converging/diverging channels are quite different, there are a number of key sections and locations which can be directly compared, such as the midsection.

Since the discharges involved in the skewed, converging and diverging channels differed, they will be compared by using similar relative depth values, namely (1)  $Dr = 0.2, 0.3$  and  $0.5$ ; (2) non-dimensional velocity ( $Ur$ ):

$$Ur = Ud / Um \quad (3)$$

where  $Ud$  = depth-averaged velocity; and  $Um$  = cross-section-averaged velocity; and (3) non-dimensional position ( $Xr$ ) defined as:

$$Xr = (X - X_{mid-section}) / L \quad (4)$$

where  $L$  = length of the non-prismatic reach.

### 5.1 Surface water profiles

Figure 10 shows a selection of water surface profiles, measured for the different geometries and flow depth. The different flow behaviours depicted in the previous sections are clearly identifiable.

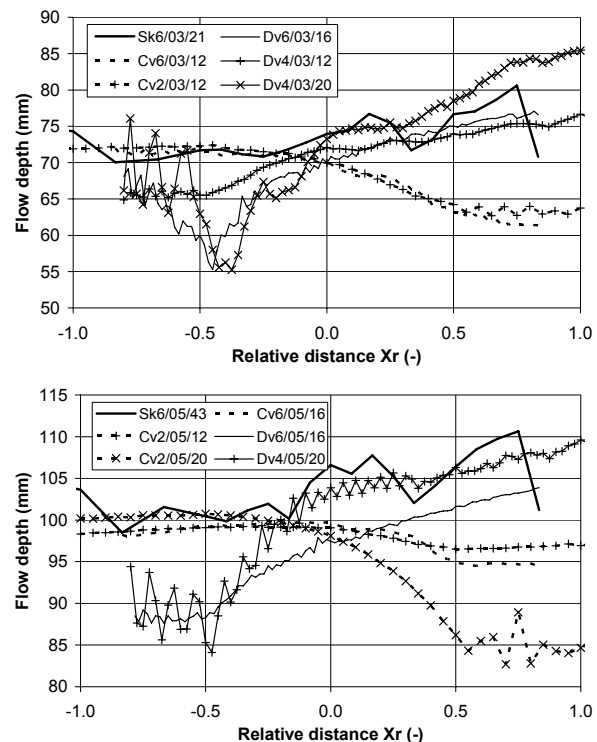


Figure 10. Water surface profiles for selected cases.  $Dr = 0.3$  and  $0.5$ . The non-prismatic sections are located in the segment  $Xr = [-0.5, 0.5]$

The flow depth slightly increases along the non-prismatic section for the skewed channel Sk6. The diverging channel (Dv4 & Dv6) also shows increasing flow depth, preceded in this case in the upstream prismatic section by a strong decrease (M2 profile). In some cases, for the larger discharges, the flow conditions were close to critical flow just at the entrance of the enlarging section. Strong surface perturbations (with quite stable waves) are observed in this area.

For the converging geometries (Cv2 & Cv6) plunging flow in the non-prismatic section was observed and the water profile is smoother than for the diverging cases. Similarities between the flow conditions for different converging angle are again notable (see e.g. Cv6/03/12 & Cv2/03/12).

### 5.2 Velocity

Figure 11 shows non-dimensional velocity  $Ur$  distribution in the mid-section for various geome-

tries, and different flow depths. For legibility, only one profile is shown for each series, taking benefit of the similarity properties demonstrated earlier.

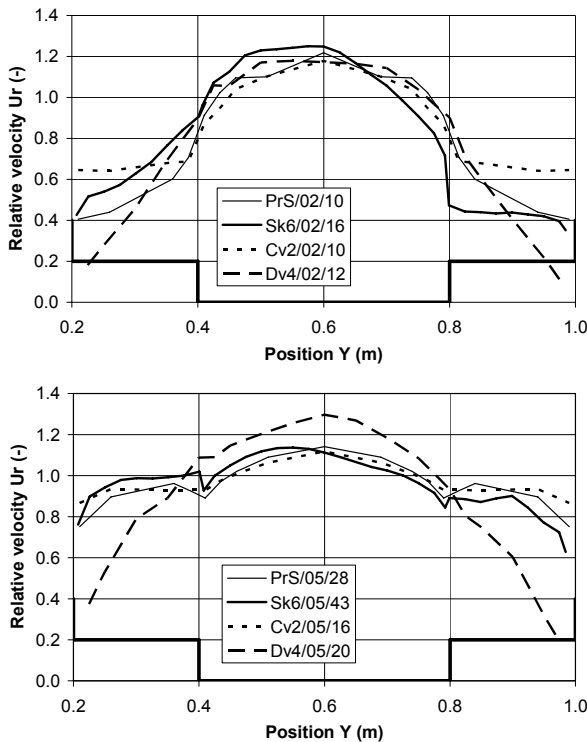


Figure 11. Non-dimensional velocity distribution for selected flow cases, in the mid-section.  $Dr=0.2$ , and  $0.5$

In the main channel, the mean velocity is almost the same for the prismatic PrS, skewed Sk6, and converging geometries Cv2 & Cv6. The skewed channel velocity profile is however less symmetrical, with its peak clearly shifted towards its enlarging floodplain ( $Y < 0.4$  m). Also, the diverging channel Dv4 profile present larger velocities in the main channel, related to the lower values on its floodplains.

The converging floodplains (Cv2, Cv6 and right side of Sk6) present a flatter profile than the prismatic channel PrS. This is related to the convergence of the flow which tends to ensure the velocity distribution becomes more uniform. The mean floodplain velocity in the converging channel is larger than in the prismatic channel, itself larger than in the skewed channel. This is believed to be related to the obstruction effect in the symmetrically converging channel, where all of the flow is forced to accelerate, whereas it can freely expand on the enlarging floodplain in the skewed channel.

On the enlarging floodplain (Dv4 and left side of Sk6), the velocity profile present an almost linear transition between a maximum velocity at the interface and a minimum velocity at the left bank ( $Y = 0.2$  m). This minimum velocity is almost equal to zero for the diverging channel case Dv4. In both cases, the velocity at the interface is found

to be larger than in the prismatic reference case: as the water is flowing from the main channel, it enters the floodplain with the main channel streamwise velocity. The mean velocity is larger in the skewed channel Sk6 than in the diverging channel Dv4. This is probably due to the forcing of the flow by the convergence on the other floodplain of the skewed channel, whereas in the diverging channel, no forcing controls the flow expansion.

Figure 12 shows the velocity profiles at the outlet of the skewed channel Sk6, compared to the profiles in the asymmetric prismatic channel PrA. Observations are very similar to those for the enlarging floodplain in the mid-section: the velocity at the interface is much larger for the skewed channel than in the prismatic case; then it decreases linearly towards the bank.

### 5.3 Discharge distribution

The evolution along the channel length of the discharge distribution between subsections was estimated from the velocity distribution for all cases.

Figure 13 shows the evolution of this distribution for selected cases at  $Dr = 0.5$ . Similar evolution is observed for almost all cases in a same series, excepted for the Dv4 series, where the lack of symmetry of the flow causes some unevenness.

On the converging floodplain (right), the discharge ratio evolution is rather similar between the converging Cv6 and skewed Sk6 channels, with a quasi-linear evolution. On the diverging floodplain (left), the discharge in the skewed channel Sk6 is found to grow faster and more linearly than in the diverging channel Dv6. This results from the forcing of the flow by the converging floodplain in the skewed case.

Figure 14 summarizes discharge distribution at mid-section for most of the investigated cases at  $Dr = 0.3$ . In agreement with the analysis of the velocity distribution, the floodplain discharge is found slightly larger in the converging cases Cv6 & Cv2 than in the prismatic cases PrS. As already pointed out, this is probably due to the flow obstruction resulting from the contraction. In the diverging cases Dv6, the discharge is lower, due to the flow expansion and to the absence of forcing.

In the skewed channel Sk6, the discharge on the expanding floodplain (left) is larger than in the prismatic case, as a result of the flow forcing by the contraction of the right floodplain. On the other hand, the contracting floodplain presents a lower discharge, as it is not obstructed.

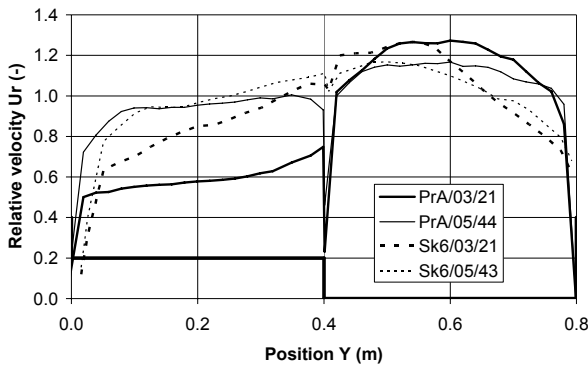


Figure 12. Non-dimensional velocity distribution for selected flow cases, in the end of non-prismatic section of Sk6

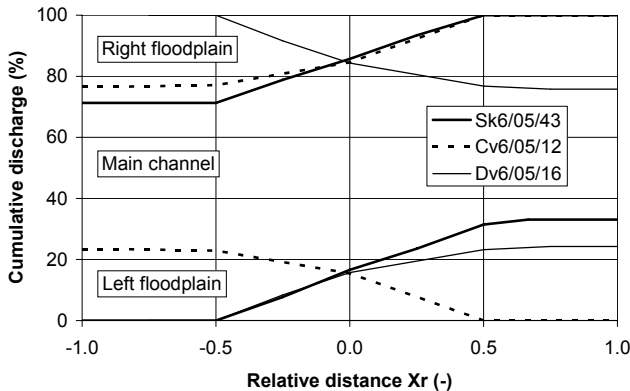


Figure 13. Discharge distribution between subsections along channel length for selected cases ( $Dr = 0.5$ )

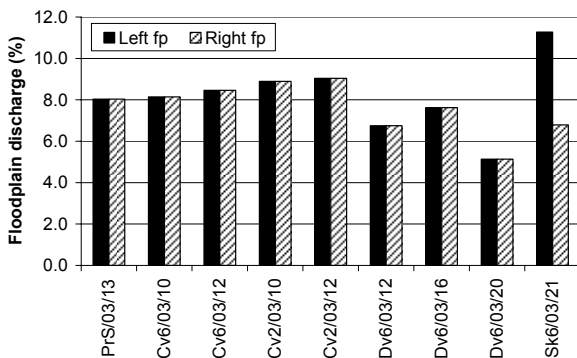


Figure 14. Floodplain discharge in mid-section ( $Dr = 0.3$ )

## 6 CONCLUSIONS

This paper summarizes the findings from three pieces of experimental research on non-prismatic compound channels, namely work carried out on converging, diverging and skewed channels. The findings of each of these studies have been briefly covered within this paper and comparisons between the datasets drawn.

Similarities between velocity profiles and discharge distribution are highlighted for the contracting floodplains of the converging and skewed channels, and for the expanding floodplains of the diverging and skewed channels. On the contracting floodplains, there is a significant homogenization of the velocity. The shear layer usually ob-

served in prismatic geometries near the interface with the main channel completely vanishes. On the expanding floodplains, the shear layer also disappears and is replaced by a linear velocity distribution, between a maximum at the interface, close to the main-channel velocity, and a minimum at the floodplain bank.

Some discrepancies are also pointed out. The floodplain discharge measured in symmetrically converging channels is larger than on the contracting floodplain of the skewed channel, due to the flow obstruction by the contraction. Conversely, the discharge is higher on the skewed channel expanding floodplains than in the symmetrically diverging case, as the contracting floodplain forces the flow to enter the opposite floodplain.

## REFERENCES

- Atabay, S. 2001. *Stage-discharge, resistance and sediment transport relationships for flow in straight compound channels*, PhD Thesis, The University of Birmingham, Birmingham, UK.
- Bousmar D. 2002. *Flow modelling in compound channels. Momentum transfer between main channel and prismatic or non-prismatic floodplains*, PhD Thesis, Université catholique de Louvain, Belgium.
- Bousmar, D. & Zech, Y. 1999. "Momentum transfer for practical flow computation in compound channels", *J. Hydr. Eng., ASCE*, 125(7), 696-706.
- Bousmar, D., Wilkin, N., Jacquemart, J.-H. & Zech, Y. 2004a. "Overbank flow in symmetrically narrowing floodplains", *J. Hydr. Eng., ASCE*, 130(4), 305-312.
- Bousmar, D., Denis, B. & Zech, Y., 2004b, "Coherent flow structures in a converging compound channel", *Proc. River Flow 2004 Conference, Naples, Italy*, 1, 423-430.
- Bousmar, D., Rivière, N., Proust, S., Paquier, A., Morel, R. & Zech, Y. 2005. "Upstream discharge distribution in compound channel flumes", *J. Hydr. Eng., ASCE*, 131(5), 408-412.
- Bousmar, D., Proust, S. & Zech, Y. 2006. "Experiments on the flow in an enlarging compound channel", *Proc. River Flow 2006 Conference, Lisbon, Portugal*, 1, 323-332.
- Chlebek, J. 2009. *Modelling of simple prismatic channels with varying roughness using the SKM and a study of flows in smooth non-prismatic channels with skewed floodplains*, PhD Thesis, The University of Birmingham, Birmingham, UK.
- Chlebek, J. & Knight, D.W. 2008. "Observations on flow in channels with skewed floodplains", *Proc. River Flow 2008 Conference, Izmir, Turkey*, 1, 519-527.
- Elliott, S.C.A & Sellin, R.H.J. 1990. "SERC flood channel facility: skewed flow experiments", *J. Hydr. Res., IAHR*, 28(2), 197-214.
- Ervine, D.A & Jasem, H.K. 1995. "Observations on flows in skewed compound channels", *J. Wat. Marit. En., ICE*, 112, 249-259.
- James, M. & Brown, B.J. 1977. *Geometric parameters that influence floodplain flow*, Report WES-RR-H-77-1, USACE, Vicksburg, USA.
- Knight, D.W. & Shiono, K. 1990. "Turbulence measurements in a shear layer region of a compound channel", *J. Hydr. Res., IAHR*, 28(2), 175-196.



- Proust, S., Rivière, N., Bousmar, D., Paquier, A., Zech, Y. & Morel, R. 2006. "Flow in compound channel with abrupt floodplain contraction", *J. Hydr. Eng., ASCE*, 132(9), 958-970.
- Rezaei, B. 2006. Overbank flow in compound channels with prismatic and non-prismatic floodplains, *PhD Thesis*, the University of Birmingham.
- Rezaei, B. and Knight, D.W. 2009. Application of the Shiono and Knight Method in compound channels with non-prismatic floodplains, *Journal of Hydraulic Research*, IAHR, Vol. 47, No 6, 716-726.
- Sellin, R.H.J., Ervine, D.A. & Willetts, B.B. 1993. "Behaviour of meandering two-stage channels", *Proc. ICE, Wat. Marit. En.*, 101, 99-111.
- Spooner, J. & Shiono, K. 2002. "Modelling of meandering channels for overbank flow", *Wat. Marit. Eng., ICE*, 156 (WM3), 225-233.